Applied Clay Science
Manuscript Draft

Manuscript Number: CLAY12715

Title: ASSESSMENT OF SURFACE ACIDITY AND BASICITY OF HYDROCALUMITES BY NITRILE ADSORPTION. FT-IR STUDIES.

Article Type: Research Paper

Keywords: Acetonitrile; Pivalonitrile; Layered double hydroxides; Hydrocalumite; FT IR spectroscopy.

Abstract: Four hydrocalumites, suitable catalysts for transesterification reaction, were synthesized by coprecipitation of chloride salts with and without using ultrasounds. Samples were aged by refluxing with and without microwaves. Results from thermogravimetry and IR experiments confirmed that the thermal decomposition of hydrocalumites occurred in a common path of successive dehydration, dehydrogenation and decomposition steps. The surface acidity and basicity of these materials were studied by infrared spectroscopy, using pivalonitrile and acetonitrile as probe molecules to be adsorbed on the samples. After pivalonitrile adsorption, the samples outgassed at room temperature evidenced very weak acidity. The amount of Lewis acid sites increased after activation of the samples at 100 °C, and after outgassing at 400 °C stronger Lewis acid sites were detected. Additionally, these samples showed strong basicity due to the O2- anions, evidenced by the formation of (CH2CN)- anions after acetonitrile adsorption at high temperature.

Research Data Related to this Submission

There are no linked research data sets for this submission. The following reason is given:
Data will be made available on request

GRAPHICAL ABSTRACT

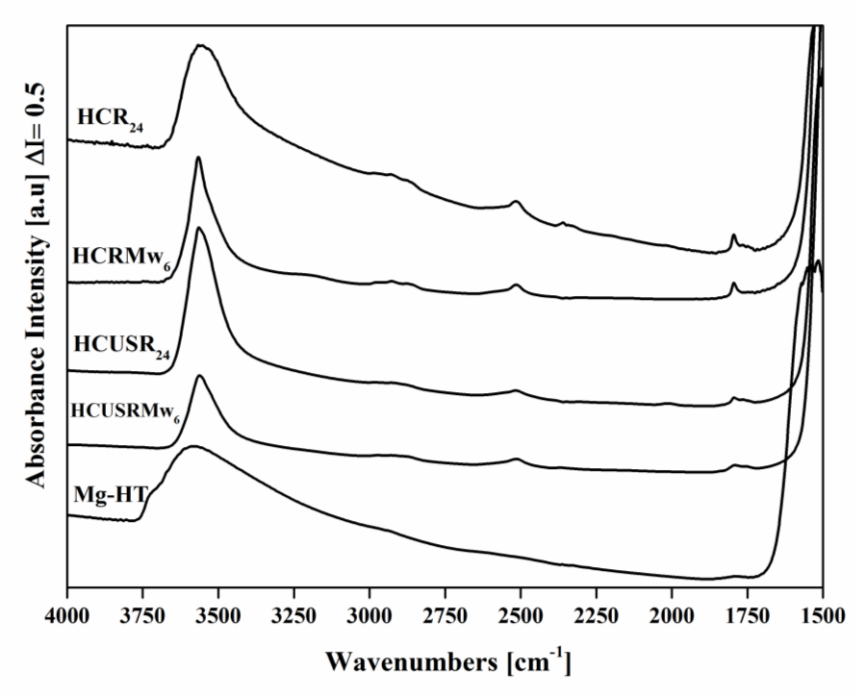

- The acidity and basicity of hydrocalumites have been studied by FT IR spectroscopy.
- Pivalonitrile and acetonitrile have been used as probe molecules for the FT IR study.
- Pivalonitrile adsorption evidenced the presence of very week acidity in the hydrocalumites.
- Acetonitrile adsorption at high temperature evidenced strong basicity in the materials.
- The use of ultrasounds for precipitation seems to enhance basicity and Lewis acidity.

ASSESSMENT OF SURFACE ACIDITY AND BASICITY OF HYDROCALUMITES BY NITRILE ADSORPTION. ~~FT-IR STUDIES~~.

Judith Granados-Reyes[a], Pilar Salagre[a], Yolanda Cesteros[a*], Guido Busca[b], Elisabetta Finocchio[b]

[a] Universitat Rovira i Virgili, Departament de Química Física i Inorgànica. C/ Marcel·lí Domingo, 1, 43007 Tarragona, Spain.

[b] Department of Civil, Chemical and Environmental Engineering, Università degli Studi di Genova, Via all'Opera Pia 15, 16145 Genova, Italy.

Abstract

Four hydrocalumites, suitable catalysts for transesterification reaction, were synthesized by coprecipitation of chloride salts with and without using ultrasounds. Samples were aged by refluxing with and without microwaves. Results from thermogravimetry and IR experiments confirmed that the thermal decomposition of hydrocalumites occurred in a common path of successive dehydration, dehydrogenation and decomposition steps. The surface acidity and basicity of these materials were studied by infrared spectroscopy, using pivalonitrile and acetonitrile as probe molecules to be adsorbed on the samples. After pivalonitrile adsorption, the samples outgassed at room temperature evidenced very weak acidity. The amount of Lewis acid sites increased after activation of the samples at 100–°C, and after outgassing at 400 °C stronger Lewis acid sites were detected. Additionally, these samples showed strong basicity due to the O^{2-} anions, evidenced by the formation of $(CH_2CN)^-$ anions after acetonitrile adsorption at high temperature.

Declarations of interest: none.

Keywords: Acetonitrile; Pivalonitrile; Layered double hydroxides; Hydrocalumite; FT IR spectroscopy.

1. Introduction

Infrared spectroscopy of adsorbed probe molecules is extensively used to study the acid and basic sites in solids. Some of the most commonly used probe molecules are pyridine, carbon monoxide, carbon dioxide, methanol, ethanol, chloroform, or ammonia, among others. Nitrile compounds, in particular, are widely used as probe molecules for the characterization of acid and basic sites (Busca, 1998; Ryczkowski, 2001; Hadjiivanov, 2014).

The adsorption of pivalonitrile (PN) is often employed for surface acidity tests (Ingemar Odenbrand *et al*., 1992). Pivalonitrile is a very weak base, sterically hindered by the ramification of the alkylic chain, whose IR spectrum is characterized by a strong band observed in the liquid phase at 2235 cm^{-1}. This band is due to the stretching of the ~~ν~~C≡N bond, and shifts to higher ~~frequency~~ when pivalonitrile interacts with electron-withdrawing centres through its nitrogen electrons lone pair (~~Ingemar~~ Odenbrand *et al*., 1992). On the other side, acetonitrile (AN) can be used to characterize both the acidity and basicity of the materials due to the hydrogen atoms of the methyl group that has a proton-donor character. The rupture of the C-H bond in the methyl groups of acetonitrile at the surface of highly basic materials results in the formation of $(CH_2CN)^-$ carbanion and/or the corresponding dimeric compound, whose IR features have been reported to fall below 2200 cm^{-1} (Lavalley, 1996; Busca, 2010).

Many studies in the last decades employed nitriles as probe molecules for zeolites, oxides and mixed oxides, to analyze their acid strength (Lavalley, 1996; Lercher *et al*., 1996; Thibault-Starzyk *et al*., 1998; Bevilacqua *et al*, 2002; Salla *et al*., 2005). Busca *et al*. (2008) studied the adsorption and desorption of acetonitrile in different inorganic solids (e.g. silicas, aluminas, metal oxides, protonated zeolites and clays). Aboulayt *et al*. (1995) studied the mechanism of acetonitrile hydrolysis on hydroxylated zirconium

dioxide and Morterra *et al*. (2002) reported the acetonitrile adsorption at room temperature in several ZnO_2-based systems for their surface characterization. There are fewer studies focused on the characterization of basic sites as well as acidic sites using nitriles. Koubowetz *et al*. (1980) studied the adsorption of acetonitrile to analyze its interactions with the atoms of MgO. Prinetto *et al*. (2004) also investigated the acid-basic properties and nature of Pd phases together with the metal-support interactions in Pd/Mg(Al)O catalysts obtained from hydrotalcites and from Ni-LDH based catalysts. These studies were performed by FTIR spectroscopy using acetonitrile and carbon monoxide as probe molecules (Prinetto *et al*. 2004; Morandi, *et al*. 2012).

Hydrotalcites are part of the family of layered double hydroxides (LDHs), being the most common compounds. Hydrocalumites (Ca/Al-LDH) are also LDHs compounds with formula $Ca_2Al(OH)_6Cl{\cdot}2H_2O$ (Forano *et al*., 2006). They are frequently applied for environmental applications such as the immobilization of toxic cations or surfactants (Zhang *et al*., 2003; Segni *et al*., 2006; Liu *et al*., 2011; Zhang *et al*., 2012). Additionally, hydrocalumites are of great interest as catalysts for organic reactions such as aldol condensation, Meerwein-Ponndorf-Verley, 1-butene isomerization and transesterification reactions, among others, due to their basic properties (Lopez-Salinas *et al*., 1996; Campos-Molina *et al*., 2010; Cota *et al*., 2010; Mora *et al*., 2010; Kuwahara *et al*., 2012). However, the acidic and basic properties of the hydrocalumites have not been deeply studied although these properties are of major interest for understanding catalytic reactions (Thibault-Starzyk *et al*., 1998).

Within this posture, the aim of this paper is to study the acidity and basicity of several hydrocalumite-type materials by infrared spectroscopy, through the adsorption of pivalonitrile and acetonitrile as probe molecules performed at several significant temperatures (Granados-Reyes, 2015). Special attention will be paid to study the effect

of using ultrasounds during precipitation and microwaves for aging compared with conventional stirring and heating methods. Additionally, several samples were tested as catalysts for the transesterification of glycerol with dimethylcarbonate to check their catalytic behavior regarding their acid-basic properties.

2. Experimental

2.1. Preparation of materials

Hydrocalumites were synthesized by the co-precipitation method. For details of the methodology please refer to Granados-Reyes *et al*. (2014). An aqueous mother solution containing $CaCl_2 \cdot 2H_2O$ (sigma-Aldrich) and $AlCl_3 \cdot 6H_2O$ (Riedel-de Haën) was prepared with a 2:1 Ca^{2+}/Al^{3+} molar ratio. The pH and the temperature were kept constant at 11.5 ± 0.1 and 60 ºC, respectively. Magnetic stirring or ultrasounds were used for mixing during precipitation. After complete addition of the metallic salts, the mother solution was aged by several treatments using microwaves or conventional heating under refluxing at different conditions as described in Table 1. Finally, all samples were filtered at room temperature, washed with deionized and decarbonated water, and then dried in an oven at 80 ºC overnight.

Table 1. Preparation conditions of hydrocalumite-type materials

Sample	Ultrasound[a]	Aging		
		Heating	T (ºC)	Time (h)
HCR_{24}	No	conventional	60	24
$HCRMw_6$	No	microwave	60	6
$HCUSR_{24}$	Yes	conventional	60	24
$HCUSRMw_6$	Yes	microwave	60	6

[a] during precipitation

2.2. FT-IR spectroscopy analysis of the samples

Infrared spectra were recorded on a NICOLET 380 FT-IR spectrometer. Spectra were acquired by accumulating 100 scans at 2 cm^{-1} resolution in the range of 400–4000 cm^{-1}. Samples were prepared by mixing the powdered solids with pressed KBr disks in a mass ratio of 1:100.

2.3. FT-IR in situ study of thermal decomposition.

Pure powder disks of the hydrocalumite materials have been outgassed at increasing temperatures up to 400–°C in the IR cell directly connected to oven and gas manipulation apparatus. Spectra were recorded at room temperature immediately after the heating step on a NICOLET 380 FT-IR spectrometer with DTGS detector and KBr beamsplitter. Spectra were acquired by accumulating 100 scans at 4 cm^{-1} resolution (OMNIC software).

2.4. FT-IR study of the acid strength of hydrocalumites-type materials by pivalonitrile adsorption

Pivalonitrile (PN) was used as probe molecule adsorption to study the acid strength in the samples. Pressed disks of pure material were prepared with weights among 160 and 220 mg of sample. These were activated at room temperature or at increasing temperatures up to 400–ºC under vacuum into the IR cell connected to a gas manipulation apparatus. Pivalonitrile (0.09 Torr at equilibrium) was introduced at room temperature and evacuated at the same temperature to eliminate physisorbed species. Stepwise adsorption and desorption was continued at 100 °C and 400-°C. The infrared spectra of the adsorption and desorption of pivalonitrile were subtracted, once at a time using the OMNIC software.

2.5. FT-IR Study of the basic strength of hydrocalumites-type materials by acetonitrile adsorption

Acetonitrile (AN) was used to study the basic strength of hydrocalumites by adsorption at increasing temperatures. Pressed disks were prepared of pure catalyst powder and activated by outgassing at 400 °C for 1 h in the IR cell. Once activated the sample, the acetonitrile was adsorbed on the surface of the material at room temperature. Stepwise acetonitrile adsorption was continued to 400 °C, and spectra of both adsorbed species and gas phase species were recorded. In the last step, the sample was evacuated at 400 ºC to evidence strongly adsorbed species at the catalytic surface.

2.6. Catalytic Tests

For the catalytic tests, 0.15 g of catalysts was used. Dimethyl carbonate and glycerol were mixed in a 3.5:1 weight ratio in a 50 ml round bottom glass reactor fitted with a reflux condenser and a thermocouple. The mixture was heated at 90 ºC under N_2 by conventional heating. After 3 h of reaction, the mixture was filtered and evaporated in a rotatory evaporator. 1 µl of the concentrated residue was analysed by gas chromatography. Gas chromatography analyses were performed in a SHIMADSU GC-2010 apparatus, equipped with a split injection mode and a flame ionization detector. The column was a SUPRAWAX-280 with 60 m length, a film thickness of 50 µm and an internal diameter of 0.25 mm. Glycerol conversion and selectivity to glycerol carbonate and glycidol were determined from calibration lines obtained from commercial products.

3. Results and discussion

3.1. FT-IR spectroscopy analysis of the samples

All samples showed similar IR spectra (Figure 1). The samples aged under microwaves had a band at 3636 cm^{-1} whereas for those conventionally aged this band appeared at 3638 cm^{-1}, slightly tailing towards lower ~~frequencies~~, in both cases. Additionally, all samples exhibited two bands, one complex band around 3486 cm^{-1}, and another weak band around 3205 cm^{-1}.

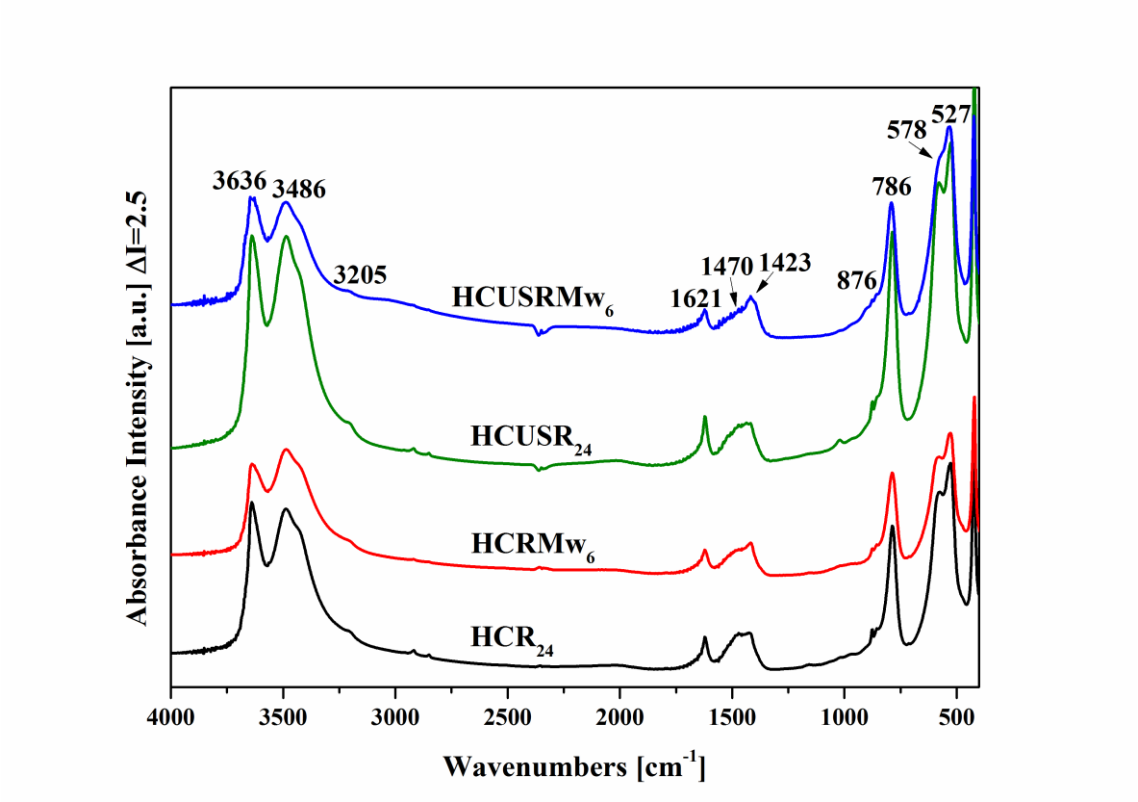

Figure 1. FT-IR skeletal spectra of the samples in the range of 4000-400 cm^{-1}.

According to Frost *et al.* (2011) the band at the highest wavenumber can be assigned to O-H stretching vibrations of hydroxyl groups in octahedral layer bonded to the cations in mixed species, such as $CaAl_2OH$ and Ca_2AlOH. The bands around 3486 cm^{-1} can be attributed to water molecules within the interlayer interacting through H-bonds, while the assignation of the band at 3205 cm^{-1} is not straightforward. Frost *et al.* (2011)

157 suggested that a band at 3365 cm^{-1} could be due to water molecules bonded to exposed
158 hydroxyl groups at the surface of the interlayer. Alternatively, such a low ~~frequency~~
159 band could be assigned to water molecules bound to carbonate ions.
160 The most characteristic vibrations of CO_3^{2-} and H_2O molecules can be observed in the
161 region between 2000-1100 cm^{-1} for all samples. The first band, around 1470 cm^{-1},
162 corresponds to the antisymmetric stretching vibration mode of carbonate (υ_3) bonded
163 hydroxyl from the brucite-like surface while the second band, around 1423 cm^{-1}, can be
164 attributed to antisymmetric stretching vibration of carbonate in calcite. However, the
165 band at 1470 cm^{-1} disappears in $HCUSR_{24}$, evidencing another component at 1508 cm^{-1},
166 which was masked by the stronger absorption, whereas in sample $HCUSRMw_6$ all these
167 components were detectable, possibly due to the presence of carbonate in several
168 different coordination at the interlayer surface. Additionally, a sharp ~~peak~~ at 1621 cm^{-1}
169 appeared for all samples, assigned to the HOH bending mode of the interlayer water
170 These results confirm the presence of carbonates although bands were very weak.
171 Moreover, the calcite phase ($CaCO_3$) was not detected in any case by XRD (Granados-
172 Reyes *et al*., 2014). Thus, low amounts of carbonates were in the samples despite of
173 using decarbonated/deionized water and an inert atmosphere during preparation to
174 prevent their formation.
175 In the range of 1000 to 400 cm^{-1} we can observe a very weak ~~peak~~ at 876 cm^{-1} for all
176 samples except for $HCUSR_{24}$, in addition to a weak ~~peak~~ around 853 cm^{-1}. These ~~peaks~~
177 correspond to the carbonate symmetric vibration out of plane bending (υ_2). Additionally,
178 the spectra show a weak band around 786 cm^{-1} that can be attributed to water
179 vibrational mode. Metal-OH bands were recorded in the infrared region between 700
180 cm^{-1} and 400 cm^{-1}. Finally, Figure 1 also exhibits three bands around 578 cm^{-1}, 527 cm^{-1}

and 423 cm^{-1} for all samples that can be assigned to Metal-O lattice vibrations ($\upsilon_{M\text{-}OH}$, $\upsilon_{M\text{-}O\text{-}M}$ and $\upsilon_{O\text{-}M\text{-}O}$).

3.2. In situ thermal decomposition studies of hydrocalumite-based materials.

The spectra of pure powder HCR_{24} sample submitted to outgassing at increasing temperature are shown in Figure 2 as an example of the hydrocalumite thermal evolution spectra in dynamic conditions.

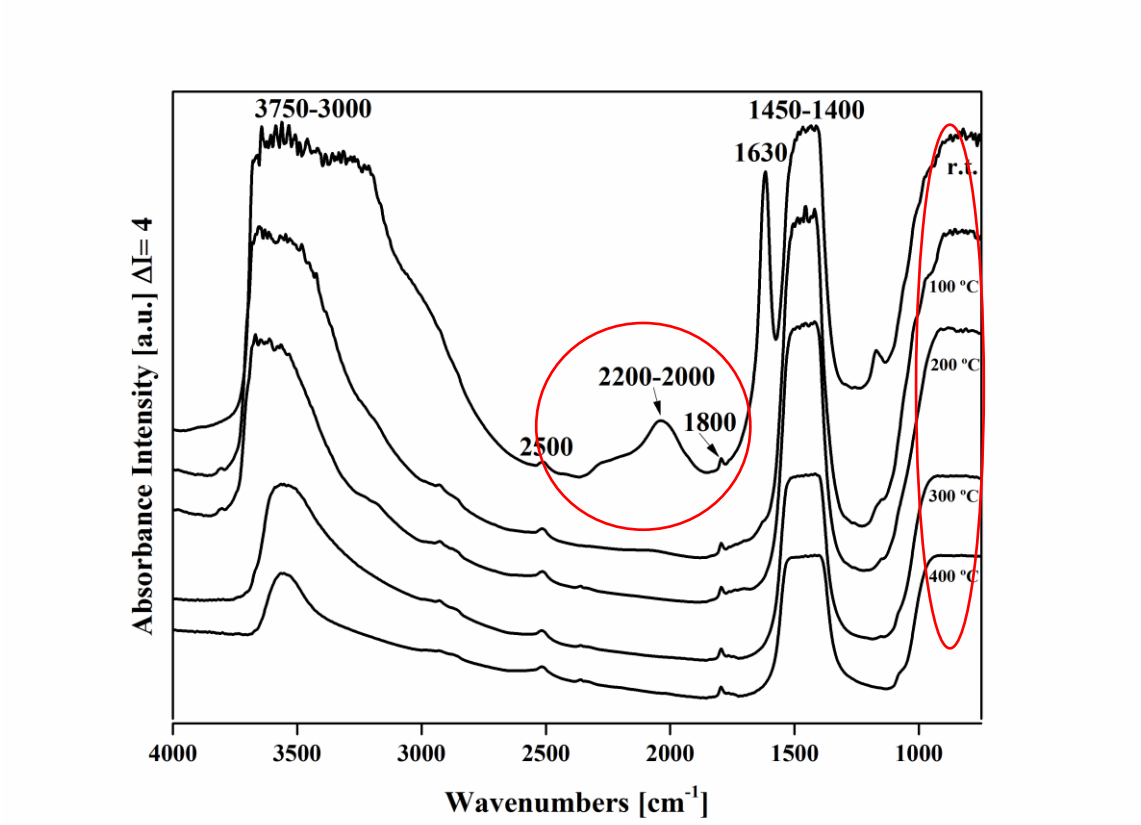

Figure 2. FT-IR spectra of pure powder HCR_{24} recorded at increasing temperatures (from top to bottom: room temperature, 100 °C, 200 °C, 300 °C, 400 °C).

Clearly, the spectrum recorded at room temperature had, as main features, the bands due to carbonate bulk species, characterized by strong and ill-resolved absorption about 1450-1400 cm^{-1} and the corresponding overtones at about 1800 and 2500 cm^{-1}, and

bands due to adsorbed water, characterized by the sharp and strong deformation mode at 1630 cm^{-1} and by a broad and weaker band in the range 2200-2000 cm^{-1}, due to overtones. Correspondingly, the OH stretching region was composed by a broad absorption extending from 3750 to 3000 cm^{-1} due to surface OH groups and adsorbed water interacting through H-bonds. A very weak and diffuse absorption centred at 3000 cm^{-1} has been previously assigned to stretching vibrational modes of water molecules in the interlayer, interacting with the chloride anions (Kloprogge and Frost, 1999). Increasing the pretreatment temperature at 100–°C resulted in the desorption of molecularly adsorbed water, thus to the disappearance of the band at 1630 cm^{-1} and the weakening of the broad bands in the range 3750-3000 cm^{-1}. This step should correspond to the first weight loss recorded by TG analysis for these materials, therefore, to the loss of physically adsorbed water and the loss of almost all interlayer water molecules, which was complete around 200-°C (Granados-Reyes *et al*., 2014). Correspondingly, in the high ~~frequency~~ region of the spectrum we were able to discriminate several components in the OH absorption band, also detectable after heating at 200-°C. Maxima can be observed at 3180 cm^{-1}, 3550 cm^{-1}, and 3650 cm^{-1}, assigned to H-bound interlayer water, strongly bonded to M-OH groups of the hydrocalumite structure.

Further heating in the 200-400–°C range led to the disappearance of all the high ~~frequency~~ components and to the formation of a weak and broad band centred at 3550 cm^{-1}. This interval corresponds to the second weight loss detected by TG and assigned to the dehydroxylation of the Ca–Al hydroxide layer. At 400–°C the collapse of the lamellar structure of hydrocalumite to oxide phases (CaO and mayenite) is likely to occur.

Nevertheless, bands due to carbonate species were still the main features of the spectrum at all the temperatures considered. Indeed, massive decarbonation of similar

materials has been reported to occur at temperatures higher than 700 °C (Vieira *et al.*, 2009).

The careful comparison of several materials after the same treatment in vacuum at 400 °C highlights few subtle differences (Figure 3). The high ~~frequency~~ absorption assigned to OH stretching modes is sharper and only slightly asymmetric in the spectra of samples treated with microwaves ($HCRMw_6$ and $HCUSRMw_6$): this effect can evidence that a limited and homogeneous amount of hydroxyl groups is formed during decomposition to the expected mixture of Ca/Al oxide phases.

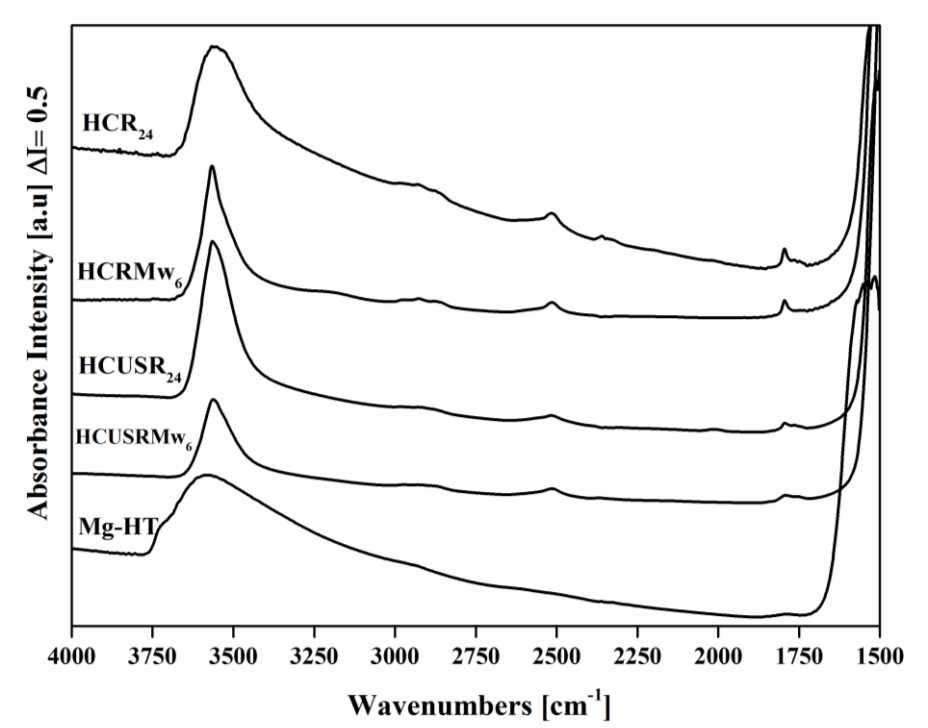

Figure 3. FT-IR spectra of pure powder hydrocalumites recorded after outgassing at 400 °C. Bottom spectrum: reference Mg-HT.

On the other side, the use of microwaves during aging of the catalysts has been previously reported to enhance the crystallinity of the samples (Granados-Reyes *et al.*, 2014). Possibly the increased crystallinity of the fresh material is partly retained also in the oxide phases after the collapse of the hydrocalumite structure. XRD of the sample

heated at 450 °C in flowing nitrogen has shown also the formation of small amount of CaO and the crystallization of the mayenite phase (Granados-Reyes. *et al.*, 2017). Spectrum of sample $HCRMw_6$ also exhibited sharp and weak bands around 2500 and 1800 cm^{-1} assigned to overtone modes of carbonate species, likely calcite phase. Longer conventional heating and ultrasound during precipitation ($HCUSR_{24}$) resulted in a strong and more complex absorption in the OH stretching region, therefore, in a highly hydroxylated surface even after heating at 400 °C in dynamic vacuum. At the same time, there was a reduction in intensity, suggesting that carbonates were slightly more prone to thermal decomposition in this sample.

After the analysis of the IR spectra recorded at increasing temperatures, we chose to carry out PN adsorption over the catalyst surfaces pretreated in vacuum at three significant temperatures: i) prolonged outgassing at room temperature (i.e. in the presence of physisorbed water and carbonates); ii) outgassing at 100 °C (i.e. removal of physisorbed water and mostly of interlayer water); iii) outgassing at 400 °C (i.e. deep dehydroxylation and likely loss of lamellar structure). Results are discussed in the following section.

3.3. Analysis of the Pivalonitrile adsorption.

Meunier et al. (2011) highlighted in a recent work the advantages in using pivalonitrile to characterize Bronsted and Lewis acidity of basic surfaces (i.e. MgO) which are indeed covered by carbonate species whose strong bands hinder the analysis with more common IR basic probes such as pyridine ~~(Meunier *et al.*, 2011)~~.

The spectra of pivalonitrile adsorbed on the hydrocalumite samples in the C≡N stretching region are reported in Figure 4. For each sample the upper spectra were those

recorded in contact with PN gas (the gas-phase spectrum was subtracted) while the lower ones (dotted line) were recorded after outgassing.

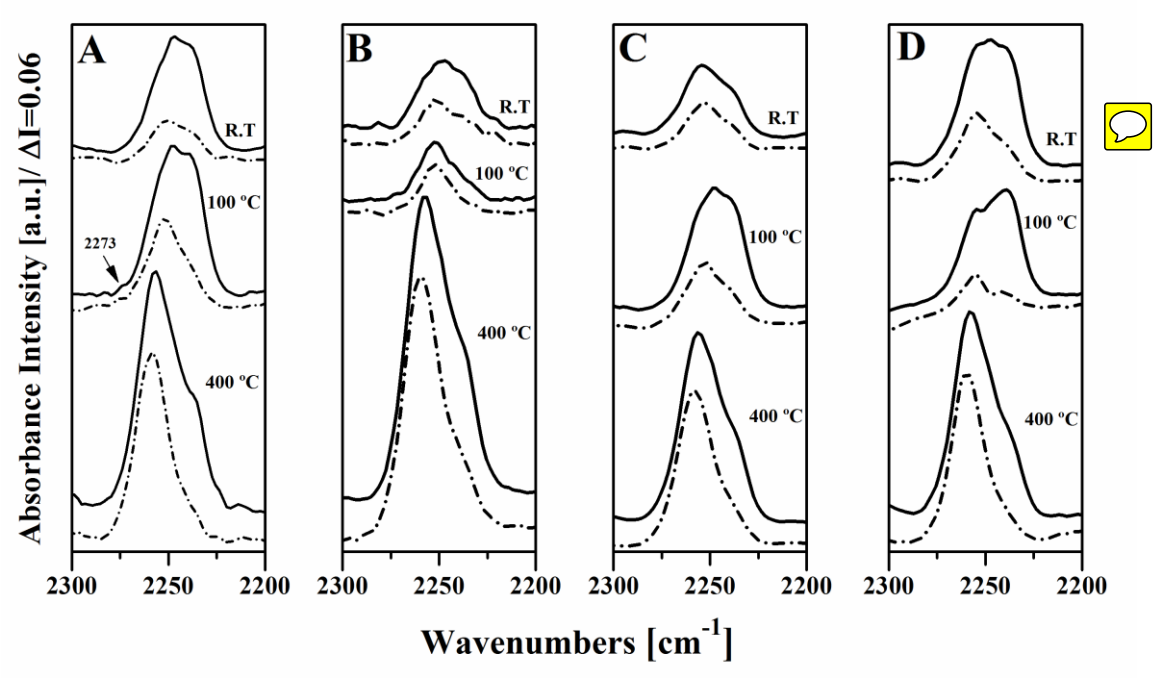

Figure 4. FT-IR subtraction spectra of the adsorbed species arising from PN adsorption (black line) and desorption (dotted line) over the samples: (A) HCR_{24}, (B) $HCRMw_6$, (C) $HCUSR_{24}$ and (D) $HCUSRMw_6$. C≡N stretching region.

From these results, by regarding the pivalonitrile adsorption spectra obtained over the samples pretreated by outgassing at room temperature (see Supporting Information, Figure S1), samples aged by conventional heating (HCR_{24} and $HCUSR_{24}$) exhibited a broad and complex band with two maxima at 2247 and 2238 cm^{-1} in HCR_{24}, and at 2253 and 2240 cm^{-1} in $HCUSR_{24}$. The bands at 2238 cm^{-1}, in HCR_{24}, and 2240 cm^{-1}, in $HCUSR_{24}$ were only very slightly shifted by the interaction with the surface in comparison with the liquid PN spectrum and can be assigned to H-bonded species over non-acidic OHs. The band at 2247 cm^{-1}, only observed in HCR_{24}, corresponded to PN interacting with very weakly acidic OH sites whereas the band at 2253 cm^{-1}, only appeared in $HCUSR_{24}$, can be related to the formation of medium-weak Lewis acid

277 sites, which may be due to exposed Ca^{2+} ions in surface defects. Samples aged by
278 microwaves ($HCRMw_6$ and $HCUSRMw_6$) showed a broad band composed by three
279 maxima. The first maximum was observed at 2238 cm^{-1}, in $HCRMw_6$ and at 2240 cm^{-1}
280 in $HCUSRMw_6$ (as for its corresponding conventional heated sample); the second
281 maximum at 2247 cm^{-1}, as in HCR_{24}; and the third maximum around 2254 cm^{-1}, as in
282 $HCUSR_{24}$. Additionally, a weak band at 2281 cm^{-1} can be observed in the $HCRMw_6$
283 sample. This band can be assigned to PN that interacts with medium-strong Lewis acid
284 sites. Moreover, it is important to note that the first maximum, related to H-bonded
285 species over non-acidic OHs, shifted to higher ~~frequency~~ values for the samples
286 prepared with ultrasounds ($HCUSR_{24}$ and $HCUSRMw_6$) when compared with those
287 synthesized by magnetic stirring (HCR_{24} and $HCRMw_6$).
288 After evacuation at room temperature, all the IR bands significantly reduced in intensity
289 and slightly changed in shape and position (Figure S1). In detail, bands below 2250 cm^{-1}
290 (i.e. the band at 2247 cm^{-1} as well as the bands around 2238-2240 cm^{-1}) almost
291 disappeared or were strongly weakened for all samples while the band above 2250 cm^{-1}
292 remained but shifted to lower ~~frequencies~~. This behaviour of the low ~~frequency~~ bands is
293 in agreement with the assignation to nitrile species weakly bound. On the other side, the
294 shift of the high ~~frequency~~ band, more resistant to outgassing as expected for nitriles
295 coordinated over Lewis sites, could be due to the low PN coverage consequent to
296 outgassing of the sample. The band around 2281 cm^{-1}, only detected in the $HCRMw_6$
297 sample spectrum at room temperature, also weakened.
298 Next, we proceed to study the pivalonitrile adsorption over the samples outgassed at
299 100 ºC (Figure 4). Figures 4-A and 4-B, show the corresponding spectra for the samples
300 stirred with magnetic stirrer, HCR_{24} and $HCRMw_6$, respectively. The two spectra were
301 similar to those obtained when the pivalonitrile was adsorbed at room temperature

(Figure S1) but they presented a new shoulder at 2273 cm^{-1}, which was indeed assigned to PN interacting with medium-strong Lewis acid sites, likely surface Al^{3+} exposed by the activation of the sample at 100 °C (or Ca^{2+} ions in a different coordination). By degassing the HCR_{24} sample, the intensity of the band around 2238 cm^{-1} decreased, the band at 2247 cm^{-1} disappeared, and a new band appeared at higher ~~frequency~~ (2252 cm^{-1}). In addition, the shoulder at 2273 cm^{-1} remained. These results indicate that higher amounts of PN were preferentially coordinated on Lewis acid sites. For the sample aged with microwaves, $HCRMw_6$, after degassing, all bands shifted to lower ~~frequencies~~ and decreased their intensity, except for that at 2251 cm^{-1}, which increased its relative intensity with respect to the other ~~peaks~~. This behaviour confirms that at 100 °C, the amount of weakly acidic OHs decreased while the amount of Lewis acidic sites increased. Additionally, after degassing, the shoulder at 2273 cm^{-1} was still detected, confirming its assignation to PN more strongly adsorbed on Lewis acid sites.

In the case of the $HCUSR_{24}$ sample, stirred with ultrasounds and aged by conventional heating, after adsorbing PN at 100 ºC, a broad band with three maxima at 2240 cm^{-1}, 2248 cm^{-1} and 2255 cm^{-1} was observed (Figure 4-C). The band at 2248 cm^{-1} was not evident in the spectrum recorded at room temperature. After degassing, this sample presented the same behaviour ~~than~~ HCR_{24}, thus, the band at 2248 cm^{-1} became the main one of the spectrum, with a shoulder at 2240 cm^{-1}.

The $HCUSRMw_6$ sample, stirred with ultrasounds and aged with microwaves, after adsorbing PN at 100 ºC, presented two bands at 2239 cm^{-1} and 2254 cm^{-1} (Figure 4-D). The relative intensity of the band at 2239 cm^{-1} increased with respect to the band at 2254 cm^{-1}, when compared to the spectrum of this sample at room temperature. This indicates that the relative amount of Lewis acid sites decreased, obtaining a higher contribution of acidity due to the OH groups. After degassing, the intensity of both

bands decreased (Figure 4-D) and the highest ~~frequency~~ band was predominant, according to its assignation to PN on Lewis acid sites.

When performing the adsorption of PN after activation of the surface at 400 °C, the same behaviour was observed for all samples. The spectra showed one main band in the range 2256-2258 cm^{-1} and a shoulder around 2237 cm^{-1} (Figure 4). A significant increase of intensity and a shift to higher ~~frequencies~~ was observed for the band appearing at 2256-2258 cm^{-1} when compared to the results obtained by adsorbing PN at 100 ºC (Figure 4). This effect can be explained by the high activation temperature of the samples. As a matter of fact, thermogravimetry (Granados-Reyes *et al*., 2014), as well as IR thermal analysis, showed that at this temperature, decomposition of the hydrocalumite structure occurs, therefore, exposing Ca and Al cations acting as Lewis acid sites. The samples aged by microwaves exhibited bands at higher ~~frequencies~~ than those aged by conventional heating suggesting an increased acidic strength of the surface sites, although strong Lewis acid sites were still not observed.

In sum, PN adsorption evidenced the increased amount of Lewis surface sites formed after thermal treatments in the range 25-100 °C, likely due to the decreasing hydroxylation degree of the surface which allows exposition of unsaturated sites. Nitriles molecules adsorbed over these sites are characterized by CN stretching bands above 2250 cm^{-1}. Some very weak absorptions around 2270 cm^{-1} could characterize stronger Lewis sites corresponding to ions in coordinatively unsaturated environment. The exposition of the hydrocalumite cations acting as Lewis sites is detected after the collapse of the hydrocalumite structure at 400 °C. At this temperature, the band due to PN on Lewis sites (CN stretching just below 2260 cm^{-1}) is the strongest in all the spectra.

3.4. Analysis of the acetonitrile (AN) adsorption.

In this section, we present the results of acetonitrile adsorption at different temperatures on the hydrocalumite samples. For each sample the spectra were recorded in contact with AN gas at the reported temperature (the corresponding gas-phase spectra were subtracted).

Figure 5 exhibits the spectra of the acetonitrile adsorption at different temperatures in the C≡N stretching region for the HCR_{24} sample.

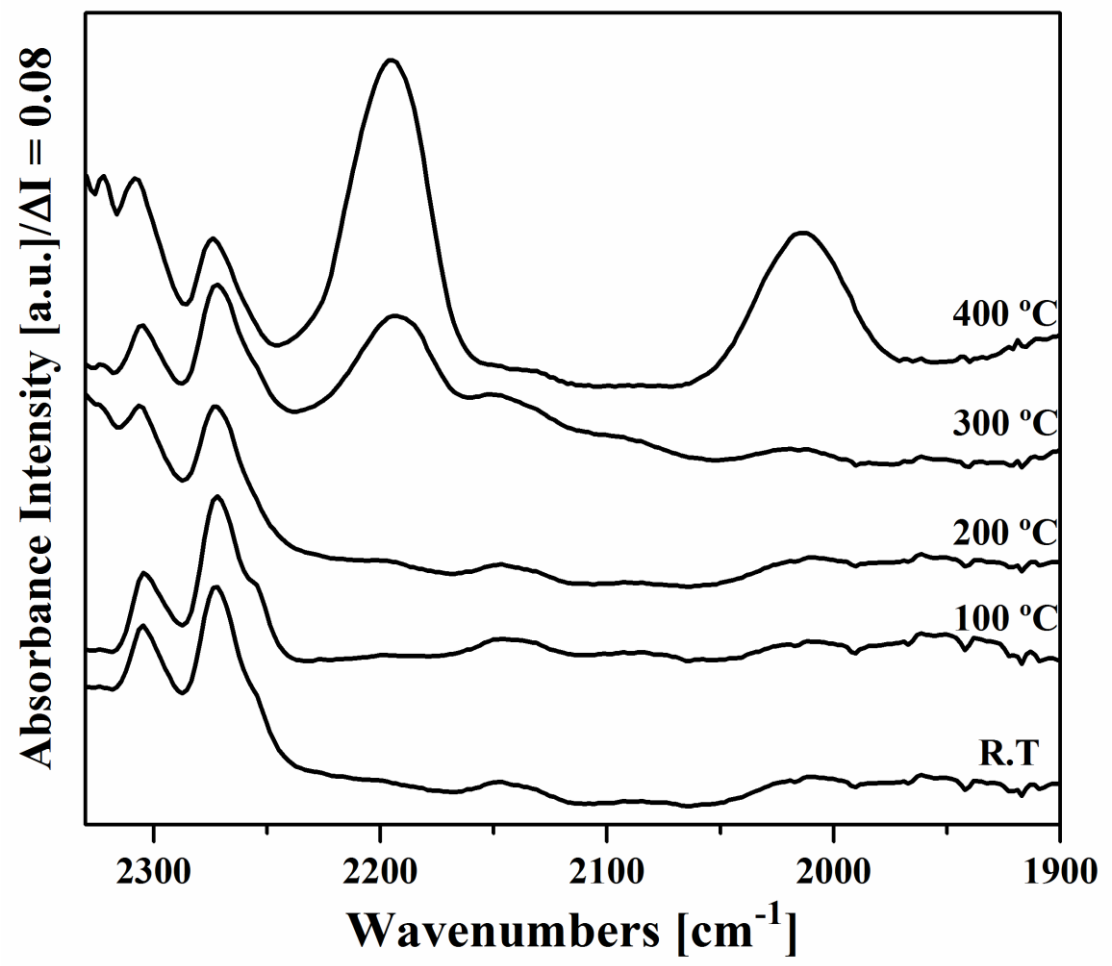

Figure 5. FT-IR subtraction spectra of Acetonitrile adsorption on the sample HCR_{24} at increasing temperatures (2350 to 1900 cm^{-1}).

In the spectra recorded from room temperature up to 200 °C the characteristic bands due to the formation of carbanions, were not observed. Only the characteristic peaks of

acetonitrile at 2272 and 2305 cm^{-1}, with a shoulder at 2255 cm^{-1} appeared. The ~~peak~~ at 2255 cm^{-1} corresponds to C≡N vibrational modes due to the formation of physisorbed species. The bands at higher ~~frequencies~~ are generated by the Fermi resonance between the C≡N stretching and a δCH_3 + υC-C combination. This doublet can be related to AN coordinated to Lewis acid sites on Al^{3+} ions (Trombetta *et al.*, 2000) partially overlapped with the doublet corresponding to AN weakly interacting with OH groups, in agreement with results from PN adsorption reported in the previous section. However, at 300 °C a new band at 2196 cm^{-1} was formed, indicating a reaction between acetonitrile and the catalyst surface (Figure 5). At 400 °C this band was even more intense and a second band appeared around 2016 cm^{-1}. These bands must be assigned to adsorbed species different than AN.

According to Lavalley (1996), the band at 2016 cm^{-1} could correspond to the $(CH_2CN)^-$ carbanion formation at the catalyst surface, stabilized by resonance, whose C≡N stretching band should fall at about 2050 cm^{-1} depending on the exposed cations. The band appeared at higher ~~frequency~~ (2196 cm^{-1}) could be related to the anion formed by dimerization of AN, through the reaction of the same carbanion discussed above. The υC≡N ~~frequency~~ of such species has been reported at about 2110 cm^{-1} and the corresponding υNH ~~frequency~~ was around 3260 cm^{-1} (Lavalley, 1996). Prinetto *et al.* (2004) also detected similar species after AN adsorption at room temperature over Mg(Al)O mixed oxides and MgAl layered double hydroxides. They assigned the band at 2088 cm^{-1} to $(CH_2CN)^-$ anions coordinated over Mg ions whereas the band characteristic of polyanions was reported at 2161 cm^{-1}, with a shoulder at lower ~~frequencies~~ (Prinetto *et al.* 2004; Morandi, *et al.* 2012). They also suggested that the preferential formation of anions or polyanions depends on the AN partial pressure at the catalyst surface, i.e. on the AN coverage, polyanions forming only in the presence of an

excess of AN. This effect will explain the detection of dimeric species as first adsorbed species in our experimental conditions, where the catalyst surface is saturated with AN. It is worth noting that upon AN adsorption the $HCUSR_{24}$ sample (Figure 6) presented the same behaviour as that described above for the HCR_{24} sample, for instance: the appearance at high temperature of two bands at 2200 ca. and just above 2000 cm^{-1} due to AN transformation products.

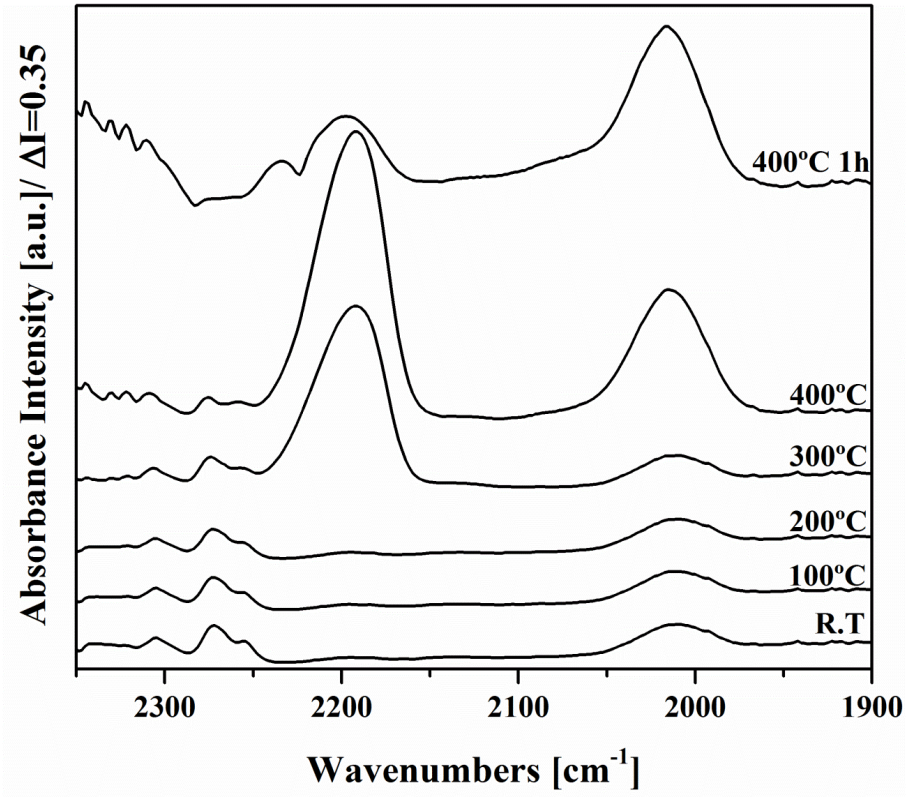

Figure 6. FT-IR subtraction spectra of Acetonitrile adsorption on the sample $HCUSR_{24}$ at increasing temperatures (2350 to 1900 cm^{-1}).

Moreover, the spectra of sample $HCUSR_{24}$ exhibited more intense ~~peaks~~ assigned to adsorbed anions than the HCR_{24} sample at 400 ºC. Actually, a weak and broad adsorption about 2000 cm^{-1} can ~~be already~~ detected after AN adsorption at room temperature, increasing in intensity above 300°C. Therefore, the precipitation of the starting salts in ultrasonic bath should help obtaining a higher basicity in the final

material. During these experiments, the adsorption contact time at 400 °C was raised up to 1 h to observe possible changes in the spectrum. In fact, a reduction in the intensity of the band around 2200 cm^{-1} was recorded while the band around 2000 cm^{-1} was maintained, as shown in Figure 6. Probably, the dimeric species (those firstly detected in the spectrum) are less stable (more reactive) than the adsorbed $(CH_2CN)^-$ anions and this effect could be also explained by some decomposition of the sample due to the high temperature used. The above discussion points out the high basicity of these materials. The very same adsorption procedure has been applied on the other two samples and the corresponding spectra are reported in Supporting Information (Figures S2 and S3) and discussed in the following paragraphs.

The spectra of the sample magnetically stirred and aged by microwaves ($HCRMw_6$) presented a decrease in the intensity of the ~~peaks~~ at 400 ºC with respect to the $HCUSR_{24}$ sample (aged by conventional heating). However, the $HCRMw_6$ sample presents an increase in the acetonitrile adsorption with respect to the HCR_{24} sample (Figure S2). This could point out a higher reactivity towards basic probe molecules. In these spectra we also detected a shoulder at 2065 cm^{-1} of the main band at 2016 cm^{-1}. The complexity of this band suggests an increase in the heterogeneity of the surface, exposing different cationic sites available to the carbanion coordination.

Finally, the sample stirred by ultrasounds and aged by microwaves ($HCUSRMw_6$) presented a different behaviour in comparison to the previous samples since there was no formation of new bands at 300 °C or 400 °C. After 1 h of adsorption at 400 °C, the formation of a very weak ~~peak~~ was observed at 2200 cm^{-1} (characterizing the dimerization of the CH_3CN). Despite maintaining the adsorption up to 3 h at 400 °C, the formation of the band around 2000 cm^{-1} was not observed. However, an increase in the intensity of the bands at 1794 cm^{-1} and 1075 cm^{-1} was recorded on longer adsorption at

400 °C (Figure S3). This could be related to the formation of acetamide type species due to nucleophilic attack of $CH_3C{\equiv}N$ with hydroxyls groups present at the surface (Lavalley, 1996). The formation of acetamide species by hydrolysis can be also responsible for the decrease of the υOH band intensity (around 3562 cm^{-1}). Therefore, the use of microwaves and ultrasounds during hydrocalumite preparation resulted in different surface characteristics of the $HCUSRMw_6$ which shows "basic" OH groups available to form acetamide specie by reaction with adsorbed AN (Meunier *et al.*, 2011). Although these basic sites were different to those observed for the rest of samples, they did not affect the catalyst activity, as later commented, since the catalytic results obtained were similar. In sum, these results confirm the formation of adsorbed anions, favoured at high temperature, which evidences the strong basicity of O^{2-} sites in these materials.

Figure 7 shows the comparison of spectra of the four hydrocalumites recorded after adsorbing AN at 400 ºC.

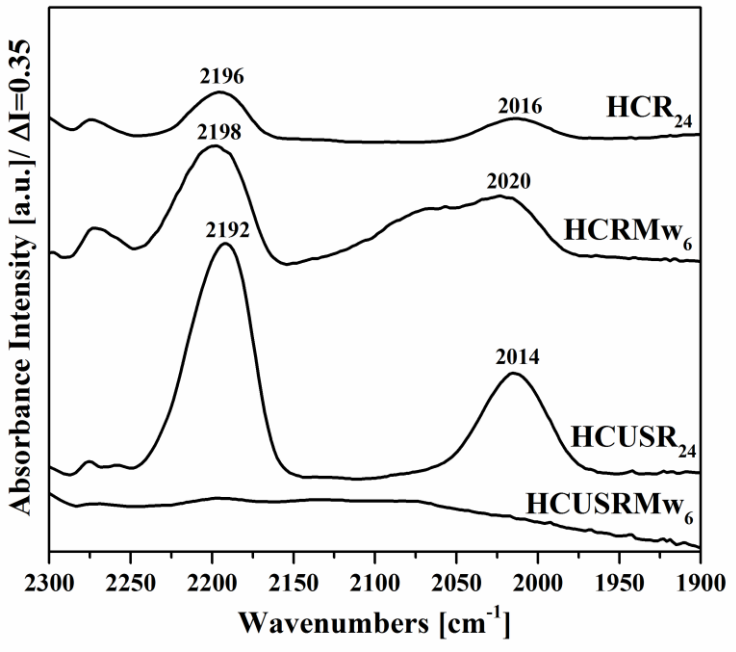

Figure 7. FT-IR subtraction spectra of surface species arising from Acetonitrile adsorption on the samples at 400 ºC in the range from 2300 to 1900 cm^{-1}.

The intensity of the band is an important factor to characterize basicity since the higher intensity involves the presence of greater amounts of basic sites. The samples show the following order regarding the $(CH_2CN)^-$ peak intensity: $HCUSR_{24}$ >$HCRMw_6$ > HCR_{24}. $HCUSR_{24}$ had the highest relative intensity of the $(CH_2CN)^-$ peak, which is also complex and possibly detectable already at room temperature. It seems that oxygen basic sites are more active in C-H bond breaking, while, at the same time, different cations are exposed at the surface, available for anions coordination. On the other side, a small shift in wavenumbers can be observed for both peaks in the different spectra, suggesting a different electronic interaction of the AN transformation products with the surface. However, the interpretation of this effect, not showing a clear trend, is not straightforward.

The reaction of glycerol transesterification with dimethyl carbonate to obtain glycerol carbonate has been used to test the catalytic behaviour of several hydrocalumite-type materials previously prepared regarding their acid-basic properties. All these samples showed medium-weak Lewis acidic sites, even after calcination, so probably the amount of undesired byproducts formed by condensation reactions of glycerol, which can polymerize in the presence of strong basic sites (Pérez-Barrado *et al*., 2015), should be limited. Some Lewis acidity can also be beneficial in the first reaction steps, i.e. reactants adsorption, considering that the oxygenated compounds can easily coordinate through the oxygen electron lone pairs to Lewis sites, likely lowering the activation energy for the following catalytic reaction. A similar effect has been proposed for other catalytic surfaces interacting with oxygen-containing reactants in dehydration reactions, such as for instance NbP catalyst for furfural production (Gomez *et al*., 2015). On the other side, the high basicity of these materials is indeed required for the transesterification catalytic activity (Di Serio *et al*., 2006).

Catalysts $cHCR_{24}$ and $cHCRMw_6$, obtained after calcination of HCR24 and $HCRMw_6$, respectively, were found highly active in terms of glycerol conversion and selectivity to glycerol carbonate (Table 2).

Table 2. Catalytic activity of several samples

Catalyst	Glycerol Conversion	Selectivity to Glycerol Carbonate	Selectivity to Glycidol	Other Products
$cHCR_{24}$	61	58	14	28
$cHCRMw_6$	76	65	14	21
$HCUSR_{24}$	84	65	10	25

Reaction conditions: dimethyl carbonate/glycerol = 3.5:1 weight ratio; stirring 1000 rpm; N_2 atmosphere; 0.15 g of catalyst; temperature: 90 ºC; time: 3 h.

Particularly, $cHCRMw_6$ presented higher glycerol conversion and higher selectivity to glycerol carbonate than $cHCR_{24}$ (Granados-Reyes *et al*., 2017). This result can be related to the acetonitrile adsorption results since $HCRMw_6$ showed stronger band of $(CH_2CN)^-$ carbanion than HCR_{24}, after AN adsorption at 400 °C. Moreover, the fresh catalyst $HCUSR_{24}$ exhibited some carbanion formation after AN adsorption at room temperature, being the most active among the catalysts here studied (84% of glycerol conversion and 65% of selectivity to glycerol carbonate, tests at 90 °C, 3 h) pointing out the role of oxygen basicity in the catalytic activity (Granados-Reyes *et al*., 2016).

4. Conclusions

Characterization by FT IR spectroscopy of the materials as prepared evidenced the typical skeletal bands of the hydrocalumite-type materials, as well as the formation of the calcite in low amounts. The very similar composition of the hydrocalumites did not allow to further evaluate significant differences in the structure, depending on the preparation method. The thermal decomposition of these samples occurs through a

494 common path of successive steps of dehydration, dehydroxylation and layered structure
495 decomposition. PN adsorption over the samples outgassed at room temperature mainly
496 evidenced very weak acidity, possibly increased by the magnetic stirring. Ultrasounds
497 technique applied during precipitation appears to increase the amount of weak Lewis
498 acid sites, likely Ca ions, characterized by bands at 2153-2155 cm^{-1}. The amount of
499 Lewis acid sites increased after activation of the samples at 100 °C (i.e. over dehydrated
500 surface) and, after outgassing at 400 °C, stronger Lewis sites were detected (C≡N
501 stretching band detected at 2158-2159 cm^{-1}). However, at this temperature the lamellar
502 structure was practically lost. All these samples are characterized by strong basicity of
503 the O^{2-} anions, evidenced by the formation of $(CH_2CN)^-$ anions after AN adsorption at
504 high temperature. Moreover, the precipitation in ultrasound seems to further enhance
505 the basicity of the resulting hydrocalumite. The high basicity of this family of materials
506 makes them suitable for the proposed transesterification reaction.
507

508 **Acknowledgements**

509 Authors acknowledge Ministerio de Economía y Competitividad of Spain and Feder
510 Funds [CTQ2011-24610], Catalan Government for FI grant [2012FI_B00564] and to a
511 mobility grant from the Universitat Rovira i Virgili [2013AEE-34].
512

References

Aboulayt A., Binet C., Lavalley J.C., 1995. IR study of acetonitrile adsorption on hydroxylated zirconium dioxide: mechanism of acetonitrile hydrolysis. J. Chem. Soc. Faraday Trans. 91, 2913.

Bevilacqua M., Alejandre A. G., Resini C., Casagrande M., Ramirez J., Busca G., 2002. An FTIR study of the accessibility of the protonic sites of H-mordenites Phys. Chem. Chem. Phys. 4, 4575–4583.

Busca G., 1998. Spectroscopic characterization of the acid properties of metal oxide catalysts. Catal. Today, 41, 191–206.

Busca G., Montanari T., Bevilacqua M., Finocchio E., 2008. Removal and recovery of nitriles from gaseous streams: An IR study of acetonitrile adsorption on and desorption from inorganic solids. Colloids Surfaces A: Physicochem. Eng. Asp. 320, 205–212.

Busca G., 2010. Bases and basic materials in chemical and environmental processes. Liquid versus solid basicity. Chem. Rev. 110, 2217–2249.

Campos-Molina M. J., Santamaría-González J., Mérida-Robles J., Moreno-Tost R., Albuquerque M. C. G., Bruque-Gámez S., Rodríguez-Castellón E., Jiménez-López A., Maireles-Torres P., 2010. Base Catalysts Derived from Hydrocalumite for the Transesterification of Sunflower Oil Energy Fuels, 24, 979–984.

Cota I., Ramírez E., Medina F., E. Sueiras J., Layrac G., Tichit D., 2010. New synthesis route of hydrocalumite-type materials and their application as basic catalysts for aldol condensation. Appl. Clay Sci. 50, 498–502.

Di Serio M., Ledda M., Cozzolino M., Minutillo G., Tesser R., Santacesaria E., 2006. Transesterification of soybean oil to biodiesel by using heterogeneous basic catalysts. Ind. Eng. Chem. Res. 45, 3009-3014.

Forano C., Hibino T., Leroux F., Taviot-Guého C., 2006. Layered Double Hydroxides. In: Bergaya, F., Theng, B.K.G., Lagaly, G. (Eds.) Handbook of Clay Science, Elsevier, Dev. Clay Sci., Volume 1, Amsterdam, pp. 1021–1095 (Chapter 13.1).

Frost R. L., Palmer S. J., Theiss F., 2011. Synthesis and Raman spectroscopic characterisation of hydrotalcites based on the formula $Ca_6Al_2(CO_3)(OH)_{16}\cdot 4H_2O$. J. Raman Spectrosc. 42, 1163–1167.

Gomez Bernal H., Raspolli Galletti A. M., Garbarino G., Busca G., Finocchio E., 2015. NbP catalyst for furfural production: FT IR studies of surface properties. App. Cat. A: General, 502, 388-398.

Granados-Reyes J., Salagre P., Cesteros Y., 2014. Effect of microwaves, ultrasounds and interlayer anion on the hydrocalumites synthesis. Microporous Mesoporous Mater. 199, 117–124.

Granados-Reyes J. Hydrocalumite-based catalysts for glycerol revalorization. PhD thesis, 2015.

Granados-Reyes J., Salagre P., Cesteros Y., 2016. CaAl-layered double hydroxides as active catalysts for the transesterification of glycerol to glycerol carbonate. Appl. Clay Sci. 132, 216-222.

Granados-Reyes J., Salagre P., Cesteros Y., 2017. Effect of the preparation conditions on the catalytic activity of calcined Ca/Al-layered double hydroxides for the synthesis of glycerol carbonate. Appl. Catal. A: Gen. 536, 9-17.

Hadjiivanov K., 2014. Identification and Characterization of Surface Hydroxyl Groups by Infrared Spectroscopy. Adv. Catal. 57, 99–318.

Ingemar Odenbrand C.U. Brandin J.G.M., Busca. G., 1992. Surface acidity of silica-titania mixed oxides J. Catal. 135, 505–517.

561 Kloprogge J. T., Frost R. L., 1999. Fourier transform infrared and Raman spectroscopic
562 study of the local structure of Mg-, Ni-, and Co-hydrotalcites. J. Solid State Chem. 146,
563 506–515.
564 Koubowetz F., Latzel J., Noller H., 1980. Adsorption of Acetonitrile on Magnesia, an
565 IR and TPD Study. J. Colloid Interface Sci. 74, 322–330.
566 Kuwahara Y., Tsuji K., Ohmichi T., Kamegawa T., Mori K., Yamashita H., 2012.
567 Transesterifications using a hydrocalumite synthesized from waste slag: an economical
568 and ecological route for biofuel production. Catal. Sci. Technol. 2, 1842.
569 Lavalley J. C., 1996. Infrared spectrometric studies of the surface basicity of metal
570 oxides and zeolites using adsorbed probe molecules. Catal. Today, 27, 377–401.
571 Lercher, J. A., Gründling, C., Eder-Mirth. G., 1996. Infrared studies of the surface
572 acidity of oxides and zeolites using adsorbed probe molecules. Catal. Today, 27, 353–
573 376.
574 Liu Q., Li Y., Zhang J., Y. Chi, Ruan X., Liu J., Qian G., 2011. Effective removal of
575 zinc from aqueous solution by hydrocalumite. Chem. Eng. J. 175, 33–38.
576 Lopez-Salinas E., Serrano M.E.L., Jacome M.A.C., Secora I.S., 1996. Characterization
577 of synthetic hydrocalumite-type $[Ca_2Al(OH)_6]NO_3 \cdot mH_2O$: Effect of the calcination
578 temperatureJ. Porous Mater. 2, 291–297.
579 Mora M., López M.I., Jiménez-Sanchidrián C., Ruiz J.R., 2010. Ca/Al Mixed Oxides as
580 Catalysts for the Meerwein–Ponndorf–Verley Reaction. Catal. Letters, 136, 192–198.
581 Morandi S., Manzoli M., Prinetto F., Ghiotti G., Gérardin C., Kostadinova D., Tichit D.,
582 2012. Supported Ni catalysts prepared by intercalation of Layered Double Hydroxides:
583 Investigation of acid–base properties and nature of Ni phases. Microporous Mesoporous
584 Mater. 147, 178–187.

585 Morterra C., Peñarroya Mentruit M., Cerrato G., 2002. Acetonitrile adsorption as an IR
586 spectroscopic probe for surface acidity/basicity of pure and modified zirconias. Phys.
587 Chem. Chem. Phys. 4, 676–687.

588 Ni J., Meunier F.C., Robles-Manuel S., Barrault J., Valange S., 2011. Characterization
589 of Surface Acidity of Carbonated Materials by IR-Sensitive Molecular Probes:
590 Advantages of Using tert-Butyl Cyanide. J.Phys. Chem. C, 115, 24931-24936.
591 Prinetto F., Manzoli M., Ghiotti G., Martinez Ortiz M. D. J., Tichit D., Coq B., 2004.
592 Pd/Mg(Al)O catalysts obtained from hydrotalcites: investigation of acid–base properties
593 and nature of Pd phases. J. Catal. 222, 238–249.
594 Ryczkowski J., 2001. IR spectroscopy in catalysis. Catal. Today, 684, 263–381.
595 Salla I., Montanari T., Salagre P., Cesteros Y., Busca G., 2005. Fourier Transform
596 Infrared Spectroscopic Study of the Adsorption of CO and Nitriles on Na- Mordenite:
597 Evidence of a New Interaction. J. Phys. Chem. B, 109, 915–922.
598 Segni R., Vieille L., Leroux F., Taviot-Guého C., 2006. Hydrocalumite-type materials:
599 1. Interest in hazardous waste immobilization. Phys. Chem. Solids. 67, 1037–1042.
600 Thibault-Starzyk F., Travert A., Saussey J., Lavalley J., 1998. Correlation between
601 activity and acidity on zeolites: a high temperature infrared study of adsorbed
602 acetonitrile . Top. Catal. 6, 111–118.
603 Trombetta M., Busca G., Lenarda M., Storaro L., Ganzerla R., Piovesan L., Jimenez A.,
604 Alcantara-Rodrìguez M., Rodríguez-Castellón E., 2000. Solid acid catalysts from clays
605 Evaluation of surface acidity of mono- and bi-pillared smectites by FT-IR spectroscopy
606 measurements, NH_3-TPD and catalytic tests. Appl. Catal. A Gen. 193, 55–69.
607 Vieira A. C., Moreira R. L., Dias A., 2009. Raman Scattering and Fourier Transform
608 Infrared Spectroscopy of $Me_6Al_2(OH)_{16}Cl_2{\cdot}4H_2O$ (Me = Mg, Ni, Zn, Co, and Mn) and
609 $Ca_2Al(OH)_6Cl{\cdot}2H_2O$ Hydrotalcites. J. Phys. Chem. C. 113, 13358–13368.

610 Zhang M., Reardon E. J., 2003. Removal of B, Cr, Mo, and Se from wastewater by
611 incorporation into hydrocalumite and ettringite. Environ. Sci. Technol. 37, 2947–2952.
612 Zhang P., Qian G., Xu Z. P., Shi H., Ruan X., Yang J., Frost R. L., 2012. Effective
613 adsorption of sodium dodecylsulfate (SDS) by hydrocalumite (CaAl-LDH-Cl) induced
614 by self-dissolution and re-precipitation mechanism J. Colloid Interface Sci. 367, 264–
615 71.
616

Supplementary material

Figure S1. FT-IR subtraction spectra of the surface species arising from room temperature PN adsorption (black line) and desorption (dotted line) over samples: (a) HCR_{24}, (b) $HCRMw_6$, (c) $HCUSR_{24}$ and (d) $HCUSRMw_6$. C≡N stretching region

Figure S2. FT-IR subtraction spectra of Acetonitrile adsorption on the sample $HCRMw_6$ at increasing temperatures (2350 to 1900 cm^{-1}).

Figure S3. FT-IR subtraction spectra of Acetonitrile adsorption over the sample $HCUSRMw_6$ at different temperatures in the range from 4000 to 1650 cm^{-1}.

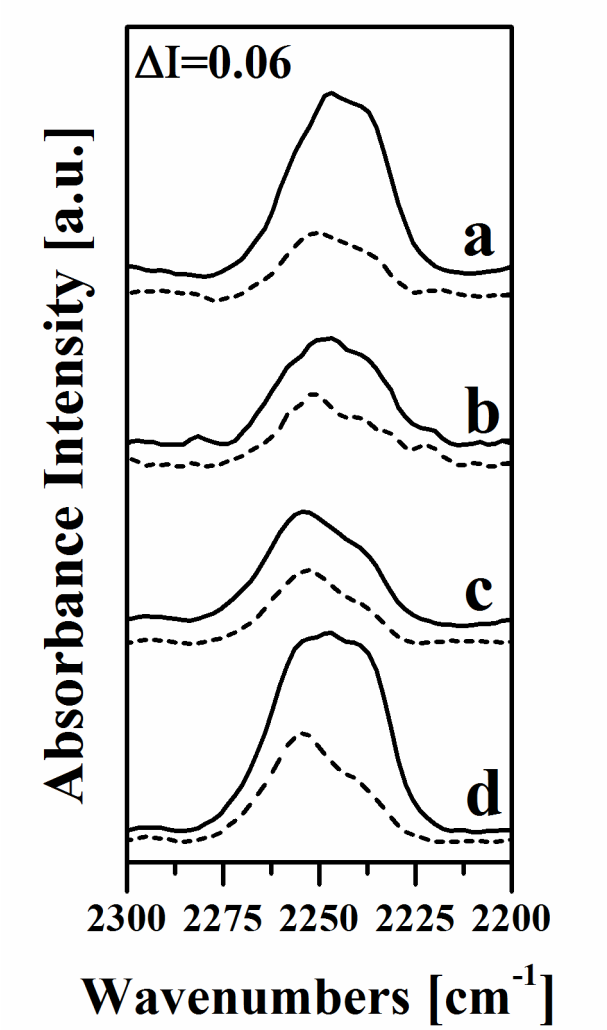

626

627 Figure S1

628

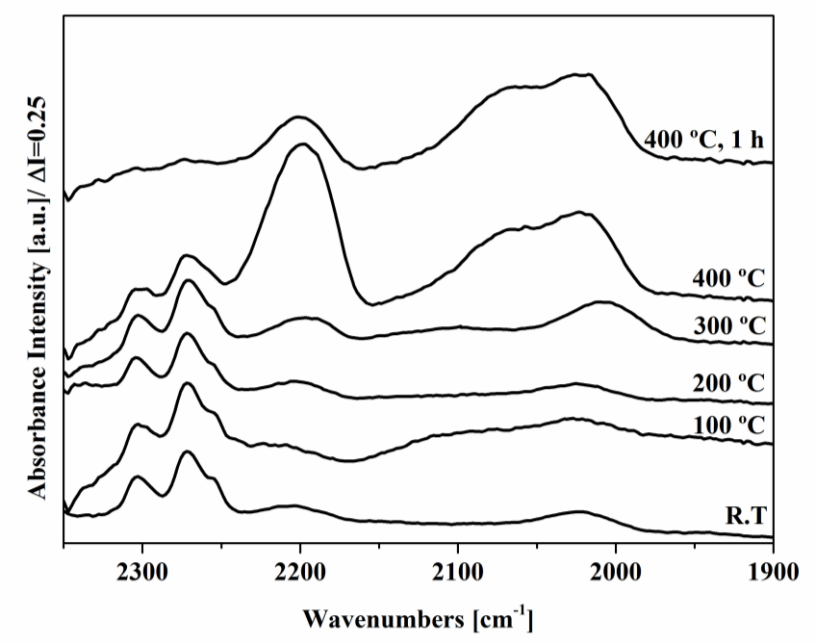

629

630 Figure S2

631

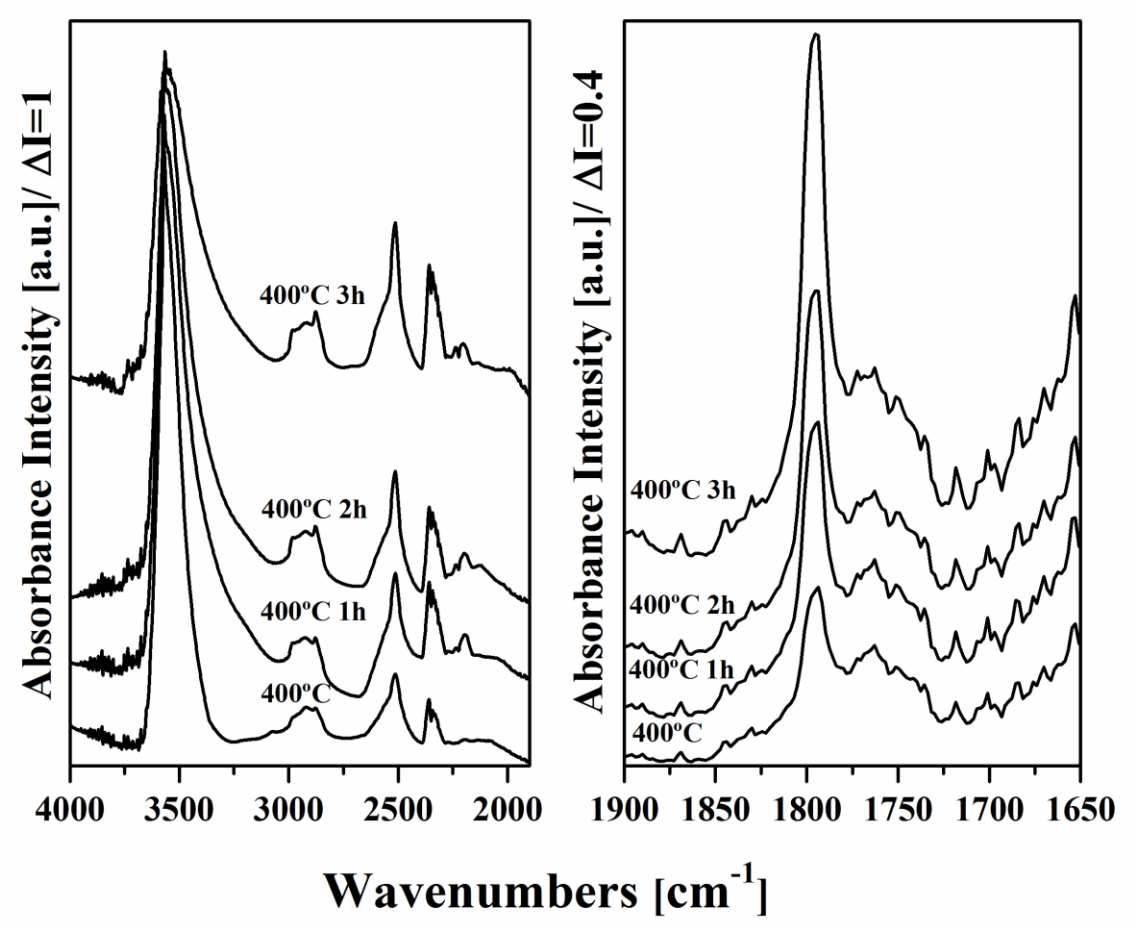

632

633 Figure S3

634